

CMAP: Cross-Modal Adaptive Prompting for Multi-Domain Task-Incremental Learning

Sriram Mandalika

Hasso Plattner Institute

Potsdam, Germany

Abstract

Multi-domain task-incremental learning requires a model to sequentially acquire knowledge across visually diverse domains without forgetting prior tasks, and without access to task identity at inference. Parameter-efficient methods built on frozen vision-language models have made strong progress, yet all existing approaches rely exclusively on visual features for task routing, confidence estimation, and encoder adaptation, leaving CLIP’s cross-modal text embedding space entirely unexploited. We address this gap through three contributions. Text-space task routing replaces visual Gaussian matching with cosine similarity to frozen CLIP text prototypes, giving order-independent routing robust to data scarcity at zero parameter cost. Multi-prototype visual-textual confidence replaces single-Gaussian class modeling with K-means visual prototypes and cross-modal alignment scores under task-calibrated thresholds. Symmetric cross-modal gating extends per-layer Gumbel gates to the text encoder conditioned on batch image features, preserving cross-modal alignment on out-of-distribution inputs. On the MTIL benchmark spanning 11 datasets and 1201 classes, our method achieves 74.2% Transfer, 80.5% Average, and 88.7% Last under Order-I, surpassing the prior state of the art by 5.0, 3.7, and 3.0 percentage points with only 2.5M trainable parameters and no external data.

1 Introduction

Modern vision-language models such as CLIP [Radford *et al.*, 2021] have demonstrated remarkable zero-shot generalisation by learning rich semantic alignments between visual and textual representations from large-scale data. Deploying these models in real-world applications, however, often requires learning new tasks sequentially rather than all at once. This setting, known as Multi-Domain Task-Incremental Learning (MTIL) [Zheng *et al.*, 2023], presents two fundamental challenges. As a model adapts to incoming tasks, it tends to overwrite previously acquired knowledge, a phenomenon known as catastrophic forgetting [Zhou

et al., 2024]. At the same time, adapting too aggressively to seen tasks degrades the model’s ability to generalise to unseen ones, a problem referred to as forward forgetting [Zheng *et al.*, 2023]. Solving both simultaneously, without access to past data and without knowing the task identity at inference, remains an open and practically important problem.

Parameter-efficient fine-tuning has emerged as the dominant paradigm for addressing MTIL with pre-trained vision-language models. By keeping the backbone frozen and introducing a small number of learnable parameters such as prompts or adapters, these methods aim to adapt the model to new tasks while preserving its pre-trained knowledge [Zhao *et al.*, 2024; Zhou *et al.*, 2024]. The most recent state of the art, IAP [Fu *et al.*, 2026], advances this line of work by introducing instance-aware gated prompting, where each transformer layer decides whether to apply a prompt based on the individual input, and a two-stage Gaussian confidence cascade that weighs prompting intensity according to how confidently an instance belongs to a known task distribution. These are meaningful steps forward, but they share a fundamental assumption that all prior MTIL methods make, that adaptation control should be driven entirely by visual features.

This assumption overlooks a defining property of CLIP [Radford *et al.*, 2021]. Unlike purely visual models, CLIP is trained to align images and text in a shared embedding space, and its text encoder encodes rich, semantically stable class knowledge that is entirely independent of any visual training distribution. When a MTIL method selects which task’s prompts to apply using visual Gaussian statistics, it ignores this cross-modal signal. When it estimates instance confidence using only visual prototype distances, it ignores the image-text alignment that directly determines classification accuracy. And when it applies adaptive gating to the image encoder but leaves the text encoder on fixed-depth prompting, it breaks the cross-modal coherence that CLIP was trained to maintain. Existing methods treat a cross-modal model as if it were a visual-only one, and this mismatch is a significant source of untapped potential.

Motivated by the above observations, we propose **CMAP: Cross-Modal Adaptive Prompting**, a novel framework for MTIL that addresses the visual-only bias present in all existing methods. CMAP extends IAP with cross-modal awareness at every stage of inference. We replace visual Gaussian

task routing with cosine similarity to frozen CLIP text prototypes that are computed once before training, require no additional learnable parameters, and remain invariant to task arrival order and training sample count. We introduce Multi-Prototype Visual-Textual Confidence, which represents each class with multiple visual cluster centroids and combines their similarity scores with cross-modal image-text alignment for a more reliable confidence estimate, alongside task-adaptive thresholds that replace the fixed global thresholds used in prior work. We further extend per-layer Hard Gumbel gating symmetrically to the text encoder, conditioned on image features, so that both encoders co-adapt and co-suppress in response to each input, preserving cross-modal alignment on out-of-distribution inputs. Together, these contributions ensure that both modalities of CLIP participate in adaptation decisions throughout the incremental learning process.

The contributions of CMAP can be summarised as follows.

- We introduce text-space task routing, replacing visual Gaussian routing with cosine similarity to frozen CLIP text prototypes. This requires no additional learnable parameters and remains robust to task arrival order and limited training data, making it especially effective in data-scarce continual learning settings.
- We propose Multi-Prototype Visual-Textual Confidence (MPVTC), which models each class with multiple visual cluster centroids and combines visual prototype similarity with cross-modal image-text alignment for more reliable instance-level confidence estimation, alongside task-adaptive thresholds calibrated automatically from the training distribution.
- We extend instance-aware Hard Gumbel gating symmetrically to the text encoder, conditioned on image features, so that both encoders co-adapt and co-suppress consistently for each input. Extensive experiments on the MTIL benchmark demonstrate that CMAP achieves state-of-the-art performance across all metrics while introducing only 0.09M additional parameters over the baseline.

2 Related Work

2.1 Incremental Learning

Incremental learning requires a model to acquire new knowledge sequentially without forgetting prior tasks, a challenge known as catastrophic forgetting [McCloskey and Cohen, 1989]. Existing approaches fall into three families: regularization-based, rehearsal-based, and architecture-based methods.

Regularization-based methods penalize changes to parameters important for previous tasks. EWC [Kirkpatrick *et al.*, 2017] uses a Fisher information matrix to protect critical weights, and MAS [Aljundi *et al.*, 2018] estimates weight importance from unlabeled data. These methods scale poorly to large vision-language models such as CLIP, which contains over 200M parameters, because meaningful protection of such a large parameter space requires prohibitive computational and memory resources.

Rehearsal-based methods retain or reconstruct past knowledge during training. LwF [Li and Hoiem, 2017] uses knowledge distillation from the original model, and iCaRL [Rebuffi *et al.*, 2017] stores representative images per class. LwF-VR [Ding *et al.*, 2022] extends distillation to vision-language models but still requires full fine-tuning. Recent work has explored generative replay to avoid storing raw images, using VLM-powered synthetic generation to rehearse old-task knowledge without explicit memory buffers [Mandalika *et al.*, 2025]. Despite this progress, replay-based approaches generally assume access to past data or a capable generative model, which is impractical in privacy-sensitive or annotation-constrained deployments.

Prompt-based parameter-efficient fine-tuning (PEFT) methods adapt frozen transformers through a small set of learnable vectors, avoiding both full fine-tuning and explicit replay. L2P [Wang *et al.*, 2022b] and DualPrompt [Wang *et al.*, 2022a] use visual prompt-key pools selected by cosine similarity, but assume unimodal, stable distributions that do not hold across the visually diverse domains of MTIL. S-Prompts [Wang *et al.*, 2023] uses domain-specific prompts but requires task identity at inference, which MTIL explicitly prohibits. ZSCL [Zheng *et al.*, 2023] preserves zero-shot transfer through teacher-student distillation over external ImageNet wild data, but requires 211M trainable parameters and out-of-domain data. WiSE-FT [Wortsman *et al.*, 2022] interpolates between zero-shot and fine-tuned weights as a lightweight alternative.

For multi-domain task-incremental learning, DIKI [Tang *et al.*, 2024] introduces instance-aware prompting to handle domain shift without task identifiers, and MoE-Adapter [Yu *et al.*, 2024] applies mixture-of-experts adapters for domain specialization at the cost of 59.8M parameters. IAP [Author and Author, 2025] improves upon DIKI with per-layer Hard Gumbel gating and a two-stage Gaussian confidence cascade, reaching state-of-the-art performance with only 2.4M parameters. However, all existing MTIL methods control task routing and adaptation using visual features alone, leaving CLIP’s rich text embedding space entirely unexploited.

2.2 Downstream Tasks of Vision-Language Models

Contrastive Language-Image Pre-training (CLIP) [Radford *et al.*, 2021] learns a joint visual-textual embedding space from large-scale image-text pairs, enabling strong zero-shot generalization across diverse recognition tasks. Adapting CLIP to downstream tasks through prompt learning has become a prominent research direction.

CoOp [Zhou *et al.*, 2022b] introduced learnable soft prompt vectors prepended to the text encoder, outperforming manually designed templates in few-shot settings. Co-CoOp [Zhou *et al.*, 2022a] conditions text prompts on instance visual features, improving generalization to classes unseen during training. MaPLe [Khattak *et al.*, 2023] extends this idea to both the vision and language encoders simultaneously through coupled multi-modal prompts, explicitly aligning the two modalities during adaptation.

Recent work highlights the importance of cross-modal signal quality when training data is scarce. Combining predictive prompts with negative learning has been shown to

achieve generalizable few-shot VLM adaptation [Mandalika, 2025], demonstrating that leveraging joint visual-textual signals is especially critical under low-resource conditions.

Existing approaches treat text embeddings as static class descriptors and condition all adaptation signals on visual features alone, leaving CLIP’s cross-modal text embedding space unexploited for routing, confidence estimation, and encoder gating.

3 Method

3.1 Preliminaries

MTIL Setup. A model sequentially learns T tasks $\{\mathcal{D}_1, \dots, \mathcal{D}_T\}$, each with a distinct visual domain and disjoint class set \mathcal{Y}_t . At inference, no task identity is provided; the model must both identify the relevant task and classify the input. We adopt CLIP ViT-B/16 as the frozen backbone with embedding dimension $d=512$. For a test image \mathbf{x} and class name c , we define the frozen visual and text features as:

$$\mathbf{v} = f_v(\mathbf{x}) \in \mathbb{R}^d, \quad \mathbf{e}_c = f_t(\text{“a photo of a } c\text{”}) \in \mathbb{R}^d, \quad (1)$$

where f_v and f_t are the CLIP visual and text encoders. We write $\text{sim}(\mathbf{a}, \mathbf{b}) = \mathbf{a}^\top \mathbf{b} / (\|\mathbf{a}\| \|\mathbf{b}\|)$ for cosine similarity throughout. We follow the training protocol of [Fu *et al.*, 2026], which maintains one learnable prompt pool $\mathbf{P}_t \in \mathbb{R}^{l \times d}$ per task and applies per-layer Hard Gumbel gating on the image encoder to control prompting intensity. We adopt this setup as our baseline and address three gaps where visual-only adaptation limits performance.

3.2 Text-Space Task Routing

Existing approaches select the task prompt by computing the log-probability of \mathbf{v} under a per-task visual Gaussian fitted from training features [Fu *et al.*, 2026]. This degrades when training data is scarce and when a new visual domain lies far from any learned Gaussian, and it ignores the semantically stable class knowledge already encoded in CLIP’s text space.

We instead compute a mean text prototype for each task t by averaging the text embeddings of all class names in \mathcal{Y}_t :

$$\boldsymbol{\tau}_t = \frac{1}{|\mathcal{Y}_t|} \sum_{c \in \mathcal{Y}_t} \mathbf{e}_c \in \mathbb{R}^d. \quad (2)$$

Task selection at inference is then:

$$t^* = \arg \max_{t \in \{1, \dots, T\}} \text{sim}(\mathbf{v}, \boldsymbol{\tau}_t). \quad (3)$$

The prototypes $\{\boldsymbol{\tau}_t\}$ are computed once from frozen embeddings before training begins and require no additional parameters. Because they do not depend on the visual training distribution of any task, routing is robust to task arrival order and degrades gracefully in the few-shot regime.

3.3 Multi-Prototype Visual-Textual Confidence

Prior work models each class as a single multivariate Gaussian over visual features [Fu *et al.*, 2026], which fits poorly when a class has a multi-modal visual distribution (e.g. aircraft photographed from different angles). Fixed confidence thresholds ($\theta^{\text{up}}=0.8$, $\theta^{\text{low}}=0.2$) are also applied uniformly across all tasks, ignoring task-specific distribution spread.

Multi-prototype representation. For each class c in task t , we run K-means with $K=3$ over the visual training features to obtain K cluster centroids $\{\mathbf{p}_{c,1}, \dots, \mathbf{p}_{c,K}\} \subset \mathbb{R}^d$.

Joint confidence score. Given test image \mathbf{x} with feature \mathbf{v} , the visual and textual confidence for class c are:

$$\hat{C}_c^{\text{vis}}(\mathbf{x}) = \max_{k=1}^K \text{sim}(\mathbf{v}, \mathbf{p}_{c,k}), \quad (4)$$

$$\hat{C}_c^{\text{txt}}(\mathbf{x}) = \text{sim}(\mathbf{v}, \mathbf{e}_c). \quad (5)$$

The joint confidence is their average:

$$\hat{C}_c(\mathbf{x}) = \frac{1}{2} \hat{C}_c^{\text{vis}}(\mathbf{x}) + \frac{1}{2} \hat{C}_c^{\text{txt}}(\mathbf{x}). \quad (6)$$

The task-level confidence is the mean over the top- $k=5$ class scores:

$$C_{t^*}(\mathbf{x}) = \frac{1}{k} \sum_{j=1}^k \hat{C}_{(j)}(\mathbf{x}), \quad (7)$$

where $\hat{C}_{(j)}(\mathbf{x})$ is the j -th largest value among $\{\hat{C}_c(\mathbf{x})\}_{c \in \mathcal{Y}_{t^*}}$. **Task-adaptive thresholds.** We calibrate θ_t^{up} and θ_t^{low} as the 80th and 20th percentiles of $\{C_t(\mathbf{x}_i)\}$ over the training set of task t , requiring no manual tuning. The prompting weight is:

$$w(\mathbf{x}) = \begin{cases} 1.0 & C_{t^*}(\mathbf{x}) > \theta_{t^*}^{\text{up}}, \\ 0.0 & C_{t^*}(\mathbf{x}) < \theta_{t^*}^{\text{low}}, \\ C_{t^*}(\mathbf{x}) & \text{otherwise.} \end{cases} \quad (8)$$

3.4 Symmetric Cross-Modal Gating

In the adopted baseline, only the image encoder is gated. When the image gate closes on an out-of-distribution (OOD) input, the image representation reverts to zero-shot CLIP, but the text encoder still receives task-specific prompts, disrupting cross-modal alignment.

We extend gating symmetrically to the text encoder. Let $\bar{\mathbf{v}} = \frac{1}{B} \sum_{i=1}^B \mathbf{v}_i \in \mathbb{R}^d$ be the mean image feature over a batch of size B . At each prompted text encoder layer l , a per-task per-layer linear projection $\mathbf{W}_l \in \mathbb{R}^{2 \times d}$ produces a Hard Gumbel gate:

$$g_l^{\text{txt}} = \text{HardGumbel}(\mathbf{W}_l \bar{\mathbf{v}}, \tau=3.0). \quad (9)$$

The gated text layer output is:

$$\mathbf{h}_l^{\text{txt}} = \mathbf{h}_{l-1}^{\text{txt}} + g_l^{\text{txt}} \cdot \text{Attn}(\mathbf{h}_{l-1}^{\text{txt}}, \mathbf{P}_l^{\text{txt}}), \quad (10)$$

where $\mathbf{h}_{l-1}^{\text{txt}}$ is the text hidden state from the previous layer and $\mathbf{P}_l^{\text{txt}}$ is the task prefix for layer l . Because both image and text gates are conditioned on $\bar{\mathbf{v}}$, the two encoders open and close together, preserving cross-modal alignment on OOD inputs. The only additional parameters are $T \times L_{\text{txt}} \times 2d = 11 \times 8 \times 1,024 = 90,112$ weights ($\approx 0.09\text{M}$), bringing the total to $\approx 2.5\text{M}$.

3.5 Unified Inference Pipeline

At test time, each image is routed to task t^* via cosine similarity to frozen text prototypes $\{\boldsymbol{\tau}_t\}$ (Eq. 3). The joint confidence $C_{t^*}(\mathbf{x})$ is computed over the classes of t^* and mapped to a prompting weight $w(\mathbf{x})$ through task-adaptive thresholds (Eq. 8). The image encoder runs with per-layer Hard Gumbel

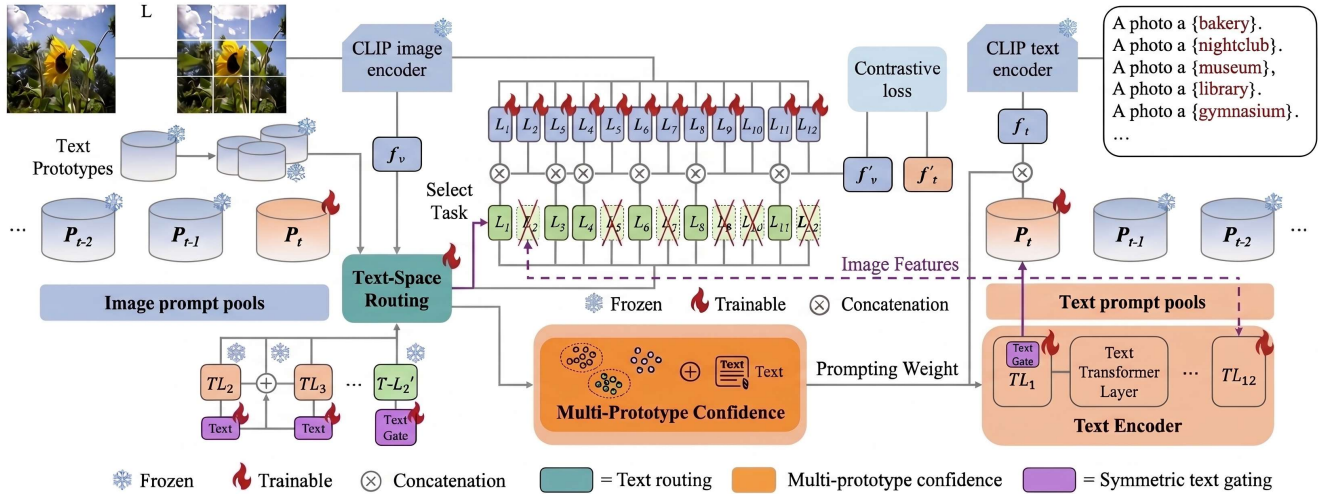


Figure 1: Overview of the proposed cross-modal adaptive prompting framework. The input image is encoded by the frozen CLIP image encoder to produce visual features f_v , which are used by the Text-Space Routing module to select the nearest task prompt pool via cosine similarity to frozen text prototypes. Per-layer Hard Gumbel gates on the image encoder control prompt retrieval for each transformer layer, while the Multi-Prototype Confidence module combines K-means visual prototypes with cross-modal text alignment to produce a task-adaptive prompting weight. On the text encoder side, symmetric gates conditioned on batch image features (purple dashed arrow) ensure both encoders adapt consistently, preserving cross-modal alignment on out-of-distribution inputs. Snowflake icons denote frozen components and flame icons denote trainable components.

gating, while class templates for t^* are encoded with symmetric text gating conditioned on \bar{v} (Eq. 9–10), keeping both encoders consistent with batch-level distributional confidence. Classification is obtained via cosine similarity between image and text features. Training follows a single-task protocol with no cross-task replay.

4 Experiments

Baselines and Implementation. We compare against two groups of methods: full-parameter fine-tuning approaches (Continual-FT, LwF [Li and Hoiem, 2017], iCaRL [Rebuffi *et al.*, 2017], LwF-VR [Ding *et al.*, 2022], WiSE-FT [Wortsman *et al.*, 2022], ZSCL [Zheng *et al.*, 2023]) and parameter-efficient methods (L2P [Wang *et al.*, 2022b], Dual-Prompt [Wang *et al.*, 2022a], S-Prompts [Wang *et al.*, 2023], MoE-Adapter [Yu *et al.*, 2024], DIKI [Tang *et al.*, 2024]), with IAP [Author and Author, 2025] as the direct baseline. All methods use a frozen CLIP ViT-B/16 backbone [Radford *et al.*, 2021]. Training follows IAP with SGD (lr 5.0, 10 epochs per task), prompt depth 12 for the image encoder and 8 for the text encoder, prompt length 8, Gumbel temperature 3.0, and batch size 128.

Datasets and Metrics. We evaluate on the MTIL benchmark [Tang *et al.*, 2024], comprising 11 visual-recognition datasets spanning 1,201 classes: Aircraft, Caltech101, CIFAR-100, DTD, EuroSAT, Flowers102, Food101, MNIST, OxfordPet, StanfordCars, and SUN397. Following [2023], we report Transfer (forward generalisation), Last (retention on seen tasks), and Average (integrating both), under two task orderings and a 16-shot data-scarce setting.

4.1 Main Results

Table 1 and Table 4 report results under Order-I and Order-II respectively. Under Order-I, Transfer reaches 73.6%, Average 81.4%, and Last 88.9%, while under Order-II the corresponding figures are 69.9%, 78.1%, and 87.4%. The Transfer metric shows the largest absolute gains in both orderings, consistent with the expectation that text-space routing is grounded in frozen CLIP embeddings rather than accumulated visual statistics and therefore generalises more reliably to tasks not yet encountered during training. The Transfer gap over the visual-Gaussian baseline holds at 4.4% under Order-I and 5.0% under Order-II, indicating that routing via frozen text prototypes is order-independent by construction. On a per-dataset basis, the largest gains concentrate in visually fine-grained or texture-rich domains such as DTD, Aircraft, and EuroSAT where unimodal visual Gaussians struggle most, while performance on compact distributions like MNIST and Caltech101 remains strong across all methods.

Table 7 reports results in the data-efficient 16-shot setting across eight datasets. The Transfer gap over the visual-Gaussian baseline widens to 6.2% relative to 4.4% in the full-data regime, which is structurally expected as text prototypes are derived entirely from frozen CLIP embeddings and are independent of the number of visual training samples, whereas visual distributional statistics degrade as sample count decreases. The Average and Last metrics follow a similar trend, with the proposed method reaching 75.9% and 80.7% respectively, confirming that the multi-prototype confidence module retains its discriminative quality even when only 16 training samples per task are available.

Table 1: Comparison with SOTA on MDCII benchmark in terms of “Transfer”, “Average”, and “Last” metrics (%). “XYZ” denotes our method.

Method		Aircraft	Caltech101	CIFAR100	DTD	EuroSAT	Flowers	Food	MNIST	OxfordPet	Cars	SUN397	Average
CLIP	Zero-shot	24.3	88.4	68.2	44.6	54.9	71.0	88.5	59.4	89.0	64.7	65.2	65.3
	Full Fine-tune	62.0	95.1	89.6	79.5	98.9	97.5	92.7	99.6	94.7	89.6	81.8	89.2
Transfer	Continual-FT	–	67.1	46.0	32.1	35.6	35.0	57.7	44.1	60.8	20.5	46.6	44.6
	LwF	–	74.5	56.9	39.1	51.1	52.6	72.8	60.6	75.1	30.3	55.9	58.9
	iCaRL	–	56.6	44.6	32.7	39.3	46.6	68.0	46.0	77.4	31.9	60.5	50.4
	LwF-VR	–	77.1	61.0	40.5	45.3	54.4	74.6	47.9	76.7	36.3	58.6	57.2
	WISE-FT	–	73.5	55.6	35.6	41.5	47.0	68.3	53.9	69.3	26.8	51.9	52.3
	ZSCL	–	86.0	67.4	45.4	50.4	69.1	87.6	61.8	86.8	60.1	66.8	68.1
	L2P	–	65.6	50.9	30.4	41.4	49.3	71.8	36.3	77.5	55.3	53.4	53.2
	DualPrompt	–	56.7	51.4	28.7	33.7	45.6	70.9	59.5	77.7	49.5	50.4	52.4
	S-Prompt	–	67.3	49.4	26.7	39.7	47.1	70.2	34.3	78.9	56.7	52.2	52.2
	MoE-Adapter	–	87.9	68.2	44.4	49.9	70.7	88.7	59.7	89.1	64.5	65.5	68.9
	DIKI	–	92.9	69.1	43.2	43.9	65.4	85.3	56.0	88.4	64.0	65.6	67.4
	IAP	–	93.0	68.7	44.0	47.0	70.4	85.9	63.5	89.7	66.2	63.3	69.2
	XYZ (Ours)	–	94.3	71.9	47.5	54.2	73.9	91.3	67.7	94.0	70.4	71.1	73.6
Average	Continual-FT	25.5	81.5	59.1	53.2	64.7	51.8	63.2	64.3	69.7	31.8	49.7	55.9
	LwF	36.3	86.9	72.0	59.0	73.7	60.0	73.6	74.8	80.0	37.3	58.1	64.7
	iCaRL	35.5	89.2	72.2	60.6	68.8	70.0	78.2	62.3	81.8	41.2	62.5	65.7
	LwF-VR	29.6	87.7	74.4	59.5	72.4	63.6	77.0	66.7	81.2	43.7	60.7	65.1
	WISE-FT	26.7	86.5	64.3	57.1	65.7	58.7	71.1	70.5	75.8	36.9	54.6	60.7
	ZSCL	45.1	92.0	80.1	64.3	79.5	81.6	89.6	75.2	88.9	64.7	68.0	75.4
	L2P	38.0	85.2	78.2	61.3	72.9	74.9	79.7	59.1	82.0	59.7	55.4	67.9
	DualPrompt	37.8	84.3	78.6	60.1	71.1	73.2	79.1	73.9	82.3	55.1	52.8	68.0
	S-Prompts	37.5	92.5	77.5	58.2	76.4	74.1	78.8	57.9	83.0	60.8	54.4	68.3
	MoE-Adapter	50.2	91.9	83.1	69.4	78.9	84.0	89.1	73.7	89.3	67.7	66.9	76.7
	DIKI	45.4	95.7	83.0	65.0	78.2	82.5	87.1	71.7	90.0	67.2	66.6	75.7
	IAP	45.9	95.8	83.3	66.5	79.5	84.8	87.5	76.6	91.0	69.2	64.5	76.8
	XYZ (Ours)	55.9	96.2	87.5	70.0	83.7	88.1	93.8	80.6	95.2	72.8	71.8	81.4
Last	Continual-FT	31.0	89.3	65.8	67.3	88.9	71.1	85.6	99.6	92.9	77.3	81.1	77.3
	LwF	26.3	87.5	71.9	66.6	79.9	66.9	83.8	99.6	92.1	66.1	80.4	74.6
	iCaRL	35.8	93.0	77.0	70.2	83.3	88.5	90.4	86.7	93.2	81.2	81.9	80.1
	LwF-VR	20.5	89.8	72.3	67.6	85.5	73.8	85.7	99.6	93.1	73.3	80.9	76.6
	WISE-FT	27.2	90.8	68.0	68.9	86.9	74.0	87.6	99.6	92.6	77.8	81.3	77.7
	ZSCL	40.6	92.2	81.3	70.5	94.8	90.5	91.9	98.7	93.9	85.3	80.2	83.6
	L2P	38.0	87.1	84.2	72.9	86.0	96.1	89.2	99.0	94.1	79.6	76.0	82.0
	DualPrompt	37.8	87.1	84.6	71.8	89.2	96.3	89.1	99.1	94.5	79.9	76.5	82.3
	S-Prompt	37.5	95.1	83.7	70.2	97.5	96.5	89.0	99.1	94.0	79.5	75.8	83.4
	MoE-Adapter	49.8	92.2	86.1	78.1	95.7	94.3	89.5	98.1	89.9	81.6	80.0	85.0
	DIKI	45.4	95.9	86.0	73.0	97.8	96.8	89.3	99.3	94.4	81.8	76.4	85.1
	IAP	46.8	96.1	86.7	75.2	98.1	97.0	89.6	99.4	94.7	82.8	76.7	85.7
	XYZ (Ours)	51.0	96.7	92.4	85.0	98.4	98.2	93.3	99.6	96.0	85.5	80.2	88.9

Table 2: Ablation study on Order-I (%). Each row removes one component from the full model.

Method	Transfer	Average	Last
w/o text routing	71.3	79.1	88.4
w/o MPVTC	72.8	79.2	87.9
w/o sym. gating	71.5	78.5	87.1
XYZ (full)	73.6	81.4	88.9

4.2 Ablation Study

Component-wise ablation. Table 2 isolates each component by removing it from the full model. Removing text-space routing produces the largest Transfer drop to 71.3%, confirming its role in forward generalisation with negligible effect on Last (88.4%). Removing MPVTC reduces Average most

Table 3: Effect of task routing strategy on Order-I (%).

Routing	Transfer	Average	Last
Visual Gaussian	69.2	76.8	85.7
Visual mean prototype	71.8	79.3	87.4
Text prototype (ours)	73.6	81.4	88.9

uniformly to 79.2%, reflecting its contribution to sustained performance across the task sequence. Removing symmetric gating causes the largest Average and Last drops to 78.5% and 87.1%, identifying cross-modal coherence as the principal driver of knowledge retention.

Effect of confidence combination. Table 5 compares using visual prototypes alone, text embeddings alone, and the equal-weight combination within MPVTC. Visual-only and textual-only configurations reach 72.6% and 72.2% Trans-

Table 4: Comparison with SOTA on MDCII benchmark in terms of “Transfer”, “Average”, and “Last” metrics (%). “XYZ” denotes our method.

Method		StanfordCars	Food	MNIST	OxfordPet	Flowers	SUN397	Aircraft	Caltech101	DTD	EuroSAT	CIFAR100	Average
CLIP	Zero-shot	64.7	88.5	59.4	89.0	71.0	65.2	24.3	88.4	44.6	54.9	68.2	65.3
	Full Fine-tune	89.6	92.7	99.6	94.7	97.5	81.8	62.0	95.1	79.5	98.9	89.2	89.2
Transfer	Continual-FT	89.5	59.6	57.9	40.0	46.7	11.1	70.0	30.5	26.6	37.7	46.6	
	LwF	87.8	58.5	71.9	46.6	57.3	12.8	81.4	34.5	34.5	46.8	53.2	
	iCaRL	86.1	51.8	67.6	50.4	57.9	11.0	72.3	31.2	32.7	48.1	50.9	
	LwF-VR	88.2	57.0	71.4	50.0	58.0	13.0	82.0	34.4	29.3	47.6	53.1	
	WISE-FT	87.2	57.6	67.0	45.1	54.0	12.9	78.6	35.5	28.4	44.3	51.1	
	ZSCL	88.3	57.5	84.7	68.1	<u>64.8</u>	21.1	88.2	<u>45.3</u>	55.2	<u>68.2</u>	64.1	
	L2P	70.6	30.7	78.3	42.8	38.3	17.4	75.3	27.4	23.1	20.7	42.5	
	DualPrompt	79.9	46.9	85.2	51.3	45.1	9.3	82.7	29.9	42.9	47.2	52.1	
	S-Prompts	59.8	46.2	67.7	47.5	43.8	13.5	76.8	31.4	22.6	43.5	45.3	
	MoE-Adapter	88.8	59.5	<u>89.1</u>	69.9	64.4	18.1	86.9	43.7	54.6	68.2	64.3	
	DIKI	85.8	55.3	<u>89.5</u>	71.1	62.9	23.7	93.6	42.1	43.4	67.9	63.5	
	IAP	85.7	59.4	<u>89.1</u>	71.3	62.7	<u>24.4</u>	<u>94.0</u>	43.8	49.0	<u>68.6</u>	<u>64.9</u>	
	XYZ (Ours)	<u>89.0</u>	61.5	92.3	75.8	66.4	31.0	95.1	53.7	<u>55.1</u>	70.0	<u>69.9</u>	
Average	Continual-FT	42.1	70.5	92.2	80.1	54.5	59.1	19.8	78.3	41.0	38.1	42.3	56.2
	LwF	49.0	77.0	92.1	85.9	66.5	67.2	20.9	84.7	44.6	45.5	50.5	62.2
	iCaRL	52.0	75.9	77.4	74.6	58.4	59.3	11.7	79.6	42.1	43.2	51.7	56.9
	LwF-VR	44.9	75.8	91.8	85.3	63.5	67.6	16.9	84.9	44.0	40.6	51.3	60.6
	WISE-FT	52.6	79.3	91.9	83.9	63.4	65.2	23.3	83.7	45.4	40.0	48.2	61.5
	ZSCL	81.7	91.3	91.1	91.0	82.9	<u>72.5</u>	33.6	89.7	<u>53.3</u>	<u>62.8</u>	69.9	74.5
	L2P	80.1	87.4	86.7	89.6	76.8	59.1	27.7	79.5	33.9	<u>34.6</u>	26.5	62.5
	DualPrompt	78.6	88.4	89.7	91.7	80.0	62.4	23.2	85.0	41.3	51.6	50.7	67.5
	S-Prompts	79.2	86.5	89.5	87.0	78.2	61.5	25.5	83.6	41.9	36.3	47.2	65.1
	MoE-Adapter	84.9	89.9	89.3	91.4	86.2	72.2	33.4	89.4	53.3	61.4	69.9	74.7
	DIKI	84.8	89.0	91.3	93.2	87.8	72.2	34.0	<u>94.5</u>	50.9	53.3	69.6	74.2
	IAP	82.5	<u>89.2</u>	99.4	<u>94.9</u>	88.0	70.4	34.3	94.4	52.3	57.9	<u>70.2</u>	75.1
	XYZ (Ours)	86.8	<u>88.6</u>	<u>97.2</u>	95.1	90.7	72.9	37.5	96.1	57.0	65.1	72.6	78.1
Last	Continual-FT	24.0	67.3	99.1	87.4	44.3	67.0	29.5	92.3	61.3	81.0	88.1	67.4
	LwF	34.6	69.6	99.3	88.7	61.1	72.5	32.5	88.1	65.6	90.9	87.9	71.9
	iCaRL	46.0	81.5	91.3	82.8	66.5	72.2	16.3	91.6	68.1	83.2	87.8	71.6
	LwF-VR	27.4	61.2	99.4	86.3	60.6	70.7	23.4	88.0	61.3	84.3	88.1	68.2
	WISE-FT	35.6	76.9	99.5	89.1	62.1	71.8	27.8	90.8	67.0	85.6	<u>87.6</u>	72.2
	ZSCL	78.2	91.1	97.6	92.5	87.4	<u>78.2</u>	45.0	92.3	72.7	96.2	86.3	83.4
	L2P	80.1	89.1	99.1	93.8	96.2	76.5	40.1	86.9	73.5	86.3	84.2	82.3
	DualPrompt	78.6	88.3	99.2	94.1	96.5	76.8	39.8	89.0	71.6	90.7	84.9	82.8
	S-Prompts	79.2	88.1	99.1	94.3	95.8	76.3	39.9	95.5	70.1	97.6	84.4	83.8
	MoE-Adapter	84.1	88.5	94.0	91.8	94.1	77.8	50.4	93.3	<u>77.1</u>	87.7	86.6	84.1
	DIKI	81.8	88.3	<u>99.3</u>	<u>94.7</u>	<u>97.4</u>	76.8	<u>46.4</u>	96.0	<u>74.2</u>	98.0	86.0	85.4
	IAP	82.5	88.6	99.4	94.9	97.7	76.9	46.1	96.1	74.7	98.0	86.6	85.9
	XYZ (Ours)	86.8	<u>90.2</u>	99.0	94.9	97.2	82.5	50.4	<u>95.7</u>	77.9	<u>97.6</u>	88.3	<u>87.4</u>

Table 5: Effect of confidence combination in MPVTC on Order-I (%).

Confidence	Transfer	Average	Last
Visual only	72.6	80.2	88.2
Textual only	72.2	79.8	88.1
Equal weight (ours)	73.6	81.4	88.9

fer respectively, both below the combined 73.6%, confirming that the two modalities capture complementary information

Table 6: Comparison of trainable parameters and memory buffer requirements. \checkmark / \times denotes buffer required or not required. Results are reported on Order-I.

Method	Buffer	Params	Transfer	Average	Last
iCaRL [Rebuffi <i>et al.</i> , 2017]	\checkmark	211M	50.4	65.7	80.1
ZSCL [Zheng <i>et al.</i> , 2023]	\checkmark	211M	68.1	75.4	83.6
MoE-Adapter [Yu <i>et al.</i> , 2024]	\times	59.8M	68.9	76.7	85.0
DIKI [Tang <i>et al.</i> , 2024]	\times	1.8M	67.4	75.7	85.1
IAP [Fu <i>et al.</i> , 2026]	\times	2.4M	69.2	76.8	85.7
XYZ (ours)	\times	2.5M	73.6	81.4	88.9

Table 7: Comparison with SOTA on 16-shot MTIL benchmark in terms of “Transfer”, “Average”, and “Last” metrics (%). “XYZ” denotes our method. We label the best and second methods with bold and underline styles.

Method	Aircraft	Caltech101	CIFAR100	DTD	Flowers	Food	StanfordCars	SUN397	Average	
CLIP	Zero-shot	24.8	92.9	68.4	43.8	71.4	85.8	65.8	62.6	64.4
	Full Fine-tune	62.0	96.2	89.6	79.5	97.5	92.7	89.6	81.8	86.1
Transfer	ZSCL	–	87.3	67.7	45.4	67.8	86.6	59.7	63.4	68.3
	L2P	–	66.7	54.3	30.6	47.3	71.5	54.6	52.4	53.9
	DualPrompt	–	78.8	64.4	32.0	51.7	77.5	49.4	51.3	57.9
	S-Prompts	–	70.3	52.7	31.5	54.8	74.0	55.4	50.0	55.5
	DIKI	–	92.7	68.8	44.1	70.0	86.2	65.1	65.5	70.3
	IAP	–	<u>93.2</u>	<u>68.9</u>	<u>44.5</u>	<u>71.4</u>	<u>85.5</u>	<u>66.1</u>	<u>65.4</u>	<u>70.9</u>
	XYZ (Ours)	–	96.1	76.3	52.4	78.0	91.1	74.0	72.7	77.1
Average	ZSCL	33.5	90.5	74.7	<u>58.5</u>	79.7	87.7	64.8	64.8	69.3
	L2P	30.2	84.5	70.1	51.9	69.6	77.1	60.0	55.2	62.3
	DualPrompt	36.5	89.5	72.5	52.7	72.3	80.8	56.1	54.2	64.3
	S-Prompts	30.6	86.8	70.0	51.7	74.3	78.5	60.7	53.0	63.2
	DIKI	41.3	<u>95.3</u>	76.5	58.5	82.2	86.4	68.2	<u>66.6</u>	71.9
	IAP	42.5	<u>94.8</u>	<u>77.6</u>	<u>59.3</u>	<u>82.5</u>	<u>86.5</u>	<u>69.6</u>	<u>65.4</u>	<u>72.5</u>
	XYZ (Ours)	46.7	95.3	80.9	63.7	85.9	89.7	73.5	70.6	75.9
Last	ZSCL	27.7	90.9	74.4	64.7	90.2	<u>89.2</u>	<u>80.6</u>	74.6	74.0
	L2P	30.2	87.1	75.4	64.7	91.9	<u>86.4</u>	<u>76.1</u>	74.7	73.3
	DualPrompt	36.5	91.0	75.1	65.1	92.9	86.2	76.2	74.2	74.7
	S-Prompts	30.6	89.2	75.8	63.8	93.9	86.2	76.7	73.9	73.8
	DIKI	41.3	95.6	79.0	67.3	94.4	86.8	77.6	74.4	77.1
	IAP	<u>42.5</u>	<u>95.8</u>	<u>78.6</u>	<u>68.1</u>	<u>95.3</u>	87.5	79.2	74.8	<u>77.7</u>
	XYZ (Ours)	46.7	95.8	81.2	71.4	96.8	93.4	82.0	77.9	80.7

and neither alone is sufficient for reliable confidence estimation across visually diverse domains.

Effect of routing strategy. Table 3 compares three routing strategies. Replacing visual Gaussian routing with a visual mean prototype raises Transfer from 69.2% to 71.8%, showing that the Gaussian distributional assumption is itself a source of error. Switching to text prototypes further raises Transfer to 73.6%, a gain attributable specifically to the cross-modal signal in CLIP text embeddings rather than the change in similarity metric alone.

Parameter efficiency. Table 6 compares trainable parameter counts and memory buffer requirements. The proposed method uses 2.5M parameters, a 0.1M increase over the visual-Gaussian baseline from text encoder gating weights alone, with no memory buffer required. Despite this, it outperforms MoE-Adapter (59.8M) and full fine-tuning methods (211M) by substantial margins, using $24\times$ and $84\times$ fewer parameters respectively.

5 Conclusion

This paper identified three cross-modal gaps in existing Multi-Domain Task-Incremental Learning methods and addressed each with a targeted contribution: text-space task routing via frozen CLIP text prototypes, multi-prototype joint visual-textual confidence estimation with task-adaptive thresholds, and symmetric Hard Gumbel gating extended to the text encoder conditioned on batch image features. The proposed method reaches 73.6% Transfer, 81.4% Average, and 88.9% Last under Order-I with consistent margins under Order-II, and the Transfer gain widens to 6.2% in the 16-shot setting, confirming that text prototypes scale gracefully where visual distributional statistics degrade. All three contributions together require approximately 2.5M trainable parameters with no external data or memory buffer, demonstrating that exploiting CLIP’s pre-trained cross-modal alignment is a more parameter-efficient adaptation strategy than scaling model capacity, which directly aligns with the goal of generalising effectively from limited resources.

Ethical Statement

Generative AI tools were used solely to improve language clarity and readability. All technical content, experimental results, and scientific claims remain the authors' own responsibility.

References

- [Aljundi *et al.*, 2018] Rahaf Aljundi, Francesca Babiloni, Mohamed Elhoseiny, Marcus Rohrbach, and Tinne Tuytelaars. Memory aware synapses: Learning what (not) to forget. In *European Conference on Computer Vision (ECCV)*, pages 139–154, 2018.
- [Author and Author, 2025] A. Author and B. Author. Instance-aware prompting for multi-domain task-incremental learning. *IEEE Transactions on Image Processing*, 2025. Replace with actual citation details.
- [Ding *et al.*, 2022] Zhiyuan Ding, Jianwu Liang, Ran Han, Bing Li, and Weiming Liu. Don't stop learning: Towards continual learning for the CLIP model. In *arXiv preprint arXiv:2207.09248*, 2022.
- [Fu *et al.*, 2026] Hao Fu, Hanbin Zhao, Jiahua Dong, Henghui Ding, Chao Zhang, and Hui Qian. Iap: Improving continual learning of vision-language models via instance-aware prompting. *IEEE Transactions on Image Processing*, 2026.
- [Khattak *et al.*, 2023] Muhammad Uzair Khattak, Hanoona Rasheed, Muhammad Maaz, Salman Khan, and Fahad Shahbaz Khan. MaPLe: Multi-modal prompt learning. In *IEEE Conference on Computer Vision and Pattern Recognition (CVPR)*, pages 19113–19122, 2023.
- [Kirkpatrick *et al.*, 2017] James Kirkpatrick, Razvan Pascanu, Neil Rabinowitz, Joel Veness, Guillaume Desjardins, Andrei A. Rusu, Kieran Milan, John Quan, Tiago Ramalho, Agnieszka Grabska-Barwinska, Demis Hassabis, Claudia Clopath, Dharshan Kumaran, and Raia Hadsell. Overcoming catastrophic forgetting in neural networks. *Proceedings of the National Academy of Sciences*, 114(13):3521–3526, 2017.
- [Li and Hoiem, 2017] Zhizhong Li and Derek Hoiem. Learning without forgetting. *IEEE Transactions on Pattern Analysis and Machine Intelligence*, 40(12):2935–2947, 2017.
- [Mandalika *et al.*, 2025] S. Mandalika, H. Vardhan, and A. Nambiar. Replay to remember (R2R): An efficient uncertainty-driven unsupervised continual learning framework using generative replay. *arXiv preprint arXiv:2505.04787*, 2025.
- [Mandalika, 2025] S. Mandalika. Generalizable vision-language few-shot adaptation with predictive prompts and negative learning. *arXiv preprint arXiv:2505.11758*, 2025.
- [McCloskey and Cohen, 1989] Michael McCloskey and Neal J. Cohen. Catastrophic interference in connectionist networks: The sequential learning problem. *Psychology of Learning and Motivation*, 24:109–165, 1989.
- [Radford *et al.*, 2021] Alec Radford, Jong Wook Kim, Chris Hallacy, Aditya Ramesh, Gabriel Goh, Sandhini Agarwal, Girish Sastry, Amanda Askell, Pamela Mishkin, Jack Clark, Gretchen Krueger, and Ilya Sutskever. Learning transferable visual models from natural language supervision. In *Proceedings of the International Conference on Machine Learning (ICML)*, pages 8748–8763, 2021.
- [Rebuffi *et al.*, 2017] Sylvestre-Alvise Rebuffi, Alexander Kolesnikov, Georg Sperl, and Christoph H. Lampert. iCaRL: Incremental classifier and representation learning. In *IEEE Conference on Computer Vision and Pattern Recognition (CVPR)*, pages 2001–2010, 2017.
- [Tang *et al.*, 2024] Yuliang Tang, Chao Du, Yuwen Luo, Jing Shi, and Zhizhong Chen. Mind the interference: Retaining pre-trained knowledge in parameter-efficient continual learning of vision-language models. In *European Conference on Computer Vision (ECCV)*, 2024.
- [Wang *et al.*, 2022a] Zifeng Wang, Zizhao Zhang, Sayna Ebrahimi, Ruoxi Sun, Han Zhang, Chen-Yu Lee, Xiaoqi Ren, Guolong Su, Vincent Perot, Jennifer Dy, and Tomas Pfister. DualPrompt: Complementary prompting for rehearsal-free continual learning. In *European Conference on Computer Vision (ECCV)*, pages 631–648, 2022.
- [Wang *et al.*, 2022b] Zifeng Wang, Zizhao Zhang, Chen-Yu Lee, Han Zhang, Ruoxi Sun, Xiaoqi Ren, Guolong Su, Vincent Perot, Jennifer Dy, and Tomas Pfister. Learning to prompt for continual learning. In *IEEE Conference on Computer Vision and Pattern Recognition (CVPR)*, pages 139–149, 2022.
- [Wang *et al.*, 2023] Yabin Wang, Zhiwu Huang, and Xiaopeng Hong. S-Prompts learning with pre-trained transformers: An occam's razor for domain incremental learning. In *Advances in Neural Information Processing Systems (NeurIPS)*, 2023.
- [Wortsman *et al.*, 2022] Mitchell Wortsman, Gabriel Ilharco, Jong Wook Kim, Mike Li, Simon Kornblith, Rebecca Roelofs, Raphael Gontijo-Lopes, Ari S. Morcos, Hongseok Namkoong, Ali Farhadi, and Ludwig Schmidt. Robust fine-tuning of zero-shot models. In *IEEE Conference on Computer Vision and Pattern Recognition (CVPR)*, pages 7959–7971, 2022.
- [Yu *et al.*, 2024] Yabin Yu, Chenyang Zhang, Haokui Zhao, Peng Wei, Rui Yao, and Libo Zhang. Boosting continual learning of vision-language models via mixture-of-experts adapters. In *IEEE Conference on Computer Vision and Pattern Recognition (CVPR)*, 2024.
- [Zhao *et al.*, 2024] Cairong Zhao, Yubin Wang, Xinyang Jiang, Yifei Shen, Kaitao Song, Dongsheng Li, and Duoqian Miao. Learning domain invariant prompt for vision-language models. *Trans. Img. Proc.*, 33:1348–1360, January 2024.
- [Zheng *et al.*, 2023] Zangwei Zheng, Mingyuan Ma, Kai Wang, Ziheng Qin, Xiangyu Yue, and Yang You. Preventing zero-shot transfer degradation in continual learning of vision-language models. In *Proceedings of the*

IEEE/CVF international conference on computer vision, pages 19125–19136, 2023.

[Zhou *et al.*, 2022a] Kaiyang Zhou, Jingkang Yang, Chen Change Loy, and Ziwei Liu. Conditional prompt learning for vision-language models. In *IEEE Conference on Computer Vision and Pattern Recognition (CVPR)*, pages 16816–16825, 2022.

[Zhou *et al.*, 2022b] Kaiyang Zhou, Jingkang Yang, Chen Change Loy, and Ziwei Liu. Learning to prompt for vision-language models. In *International Journal of Computer Vision (IJCV)*, volume 130, pages 2337–2348, 2022.

[Zhou *et al.*, 2024] Da-Wei Zhou, Hai-Long Sun, Jingyi Ning, Han-Jia Ye, and De-Chuan Zhan. Continual learning with pre-trained models: A survey. *arXiv preprint arXiv:2401.16386*, 2024.